Meteor velocity distribution from CILBO double station video camera data

Esther Drolshagen[1], Theresa Ott[1], Detlef Koschny[2], Gerhard Drolshagen[2], Bjoern Poppe[1]

[1] **University of Oldenburg, Oldenburg, Germany**
Esther.Drolshagen@uni-oldenburg.de, Theresa.Ott@uni-oldenburg.de,
Bjoern.Poppe@uni-oldenburg.de

[2] **European Space Agency, ESTEC, Noordwijk, The Netherlands**
Detlef.Koschny@esa.int, Gerhard.Drolshagen@esa.int

This paper is based on data from the double-station meteor camera setup on the Canary Islands - CILBO. The data has been collected from July 2011 until August 2014. The CILBO meteor data of one year (1 June 2013 – 31 May 2014) were used to analyze the velocity distribution of sporadic meteors and to compare the distribution to a reference distribution for near-Earth space. The velocity distribution for 1 AU outside the influence of Earth derived from the Harvard Radio Meteor Project (HRMP) was used as a reference. This HRMP distribution was converted to an altitude of 100 km by considering the gravitational attraction of Earth. The new, theoretical velocity distribution for a fixed meteoroid mass ranges from 11 - 71 km/s and peaks at 12.5 km/s. This represents the predicted velocity distribution. The velocity distribution of the meteors detected simultaneously by both cameras of the CILBO system was examined. The meteors are sorted by their stream association and especially the velocity distribution of the sporadics is studied closely. The derived sporadic velocity distribution has a maximum at 64 km/s. This drastic difference to the theoretical curve confirms that fast meteors are usually greatly over-represented in optical and radar measurements of meteors. The majority of the fast sporadics are apparently caused by the Apex contribution in the early morning hours. This paper presents first results of the ongoing analysis of the meteor velocity distribution.

1 Introduction

For this paper data is used from the CILBO (Canary Island Long-Baseline Observatory) setup on the Canary Islands. CILBO has been active since July 2011. The evaluations presented in this paper were done using the data collected in one year (1 June 2013 – 31 May 2014). During this year the system collected data for 6663 meteors which were simultaneously observed by both cameras.

The CILBO System consists of two automated stations with image-intensified video cameras named ICC (Intensified CCD camera). Each of them reach a limiting stellar magnitude of about +7.0. One camera is located on Tenerife (ICC7) and one on La Palma (ICC9), in the Canary Islands. They are pointed at the same spot in the sky at 100 km height, therefore the covered observation volumes overlap. Meteors that were observed in this overlap can be registered by both cameras making it possible to determine the trajectory of the observed meteor. Because the meteor observation is done with video cameras, a meteor is visible on a number of single frames. *Figure 1* shows the setup of the system generated with Google Earth. The system automatically checks the weather conditions during the night and only records when they allow observation. The data is saved every night and sent to a central server via ftp.

One additional camera belongs to the setup, ICC8 on Tenerife. This camera has an objective grating and records the spectrum of the brighter meteors. The meteor identification is carried out by the software MetRec (Molau, 1999). For a more detailed description of the CILBO setup see Koschny et al. (2013). Furthermore, if you want to know more about the data set and about 'lessons learnt' see Koschny et al. (2014).

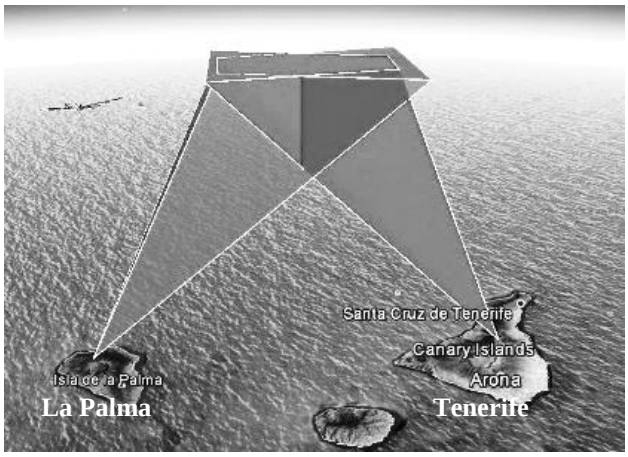

Figure 1 – Sketch of the CILBO system with the field of view of both cameras up to a height of 100 km. Additionally, the overlapping volume that is covered by both cameras is visible. La Palma with the ICC9 is on the left and Tenerife with the ICC7 is on the right.

In this paper the analysis of the CILBO data of one year is presented. Also, the theoretical velocity distribution based on the guidelines provided by the Space Environment Standard of the European Cooperation for Space Standardization (ECSS, 2008) is explained. The velocity distribution of the collected data and the bias towards higher velocities is examined.

All meteors which were simultaneously observed are separated into shower meteors and sporadics. Sporadics

are meteors which do not belong to a (known) meteor stream. The velocity distributions of the Southern Taurids and the Perseids are presented. The calculated shower velocities were found to match the literature values. The sporadic velocity distribution is relatively even distributed at the slow velocities and has a peak at 64 m/s . The majority of fast sporadics were caused by the Apex contribution in the early morning hours.

2 The ECSS distribution

The Space Environment Standard of the European Cooperation for Space Standardization (ECSS, 2008) contains the velocity distribution for the sporadic meteoroid flux at 1 AU in free space. A. D. Taylor calculated these values using parts of the data which were observed by the Harvard Radio Meteor Project (HRMP) from 1968 to 1969 (Taylor, 1995). The initial velocity distribution for meteoroids in free space, v_∞ , contains the amount of meteoroids found for certain velocities in 1 km/s bins. The standard provides a procedure to re-calculate the distribution for other heights since the velocities near Earth change due to Earth's gravitation. The normalized distribution for meteoroids in free space are plotted as the solid line in *Figure 2*. For this work the distribution at the standard altitude of 100 km will be computed. Therefore the free space values must be adapted to the reduced distance. Due to gravity, the velocity distribution of meteoroids changes in dependence of their distance to Earth. The new velocity v can be calculated using (1) and (2).

$$\boldsymbol{v^2 = v_{esc}^2 + v_\infty^2} \qquad (1)$$

$$\boldsymbol{v_{esc} = \sqrt{2 \cdot \frac{\mu}{r + H}}} \qquad (2)$$

Utilizing the velocity in free space v_∞ and the escape velocity v_{esc}. v_{esc} depends on the distance between the meteoroid and the Earth's center $r + H$. r is the mean Earth's radius ($r = 6371$ km) and H is the altitude above Earth's surface. In addition it depends on the constant $\mu = 3.986 \cdot 10^5\ km^3/s^2$, which is the product of the Earth's mass with the constant of gravitation.

The reference altitude of 100 km above Earth's surface, corresponds to a distance of $r + H = 6371$ km + 100 km = 6471 km. The corresponding meteoroid flux values were adjusted according to the velocity shift. This is done using the G factor, which shows by which a particle flux far away from Earth, is changed near to Earth. G can be computed using (3). With this factor the new shifted values $n'(v)$ of meteoroids per velocity bin can be determined from the primary values $n(v)$, using equations (3) and (4).

$$G = \frac{v^2}{v^2 - v_{esc}^2} \qquad (3)$$

$$n' = G \cdot n \qquad (4)$$

The new velocity distribution has to be re-binned and re-normalized because the shifted velocity values result in new weights for the new bins.

The velocity distributions for a distance of 100 km (dashed line) and for meteoroids in free space (solid line) were plotted in Figure 2. The integral of both curves was normalized to 1. The maximum of the meteoroid velocity distribution at 100 km is found at 12.5 km/s. The average velocities of the distributions are determined and listed in *Table 1*. The near Earth line is steeper than the velocity distribution in free space. This is a result of the acceleration of the meteoroids by the Earth gravitation. There are no meteoroids expected to be slower than 11.1 km/s which is the escape velocity v_{esc} in 100 km height. Through the process of calculating the new distribution, all contributions from the old velocities, which are smaller than v_{esc}, are collected in the first couple of bins for velocities larger than v_{esc} of the new distribution. This causes the steep increase of the curve. The physical description of this phenomenon is that, the closer the meteoroids come to the Earth, the stronger they are attracted by the Earth's gravity. Even the meteoroids with very small velocities are accelerated in the Earth's gravitation field.

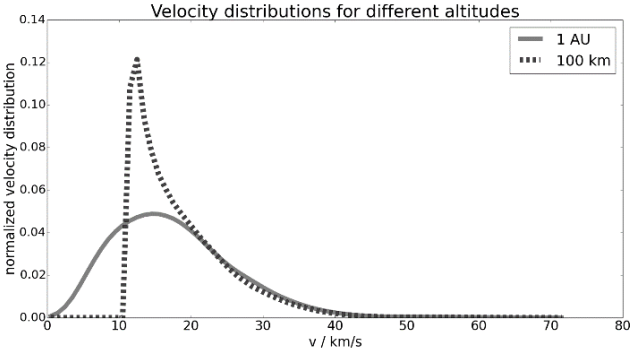

Figure 2 – Velocity distribution at 100 km above the Earth's surface (dashed line) and at 1 AU in free space (solid line).

Table 1 – Average meteoroid velocities for different altitudes above the Earth's surface.

H	$v_{avg}[km/s]$
100 km	18.47
1 AU	17.66

3 The CILBO velocity distribution

In the analyzed year (1 June 2013 – 31 May 2014) there were 6663 meteors observed simultaneously by both cameras. The information about the velocities of the double-station meteors were taken from *.daf (detailed altitude file) files which were created by a software called MOTS (Meteor Orbit and Trajectory software) (Koschny and Diaz del Rio, 2002). Furthermore, a control program has eliminated all faulty *.daf files. This are those with unphysical entries, i.e. negative velocity values or altitudes and are not used in the following. The result is 6132 double-station meteors detected simultaneously between the 1 June 2013 and the 31 May 2014. Furthermore, MOTS provides *.kml files for all double

station meteors, which can be read by Google Earth, showing the trajectory of a meteor. In *Figure 3* some exemplary meteor trajectories are shown, generated with Google Earth. For this picture the data of 9 double-station meteors recorded on the 13 December 2011 and analyzed by MOTS are utilized.

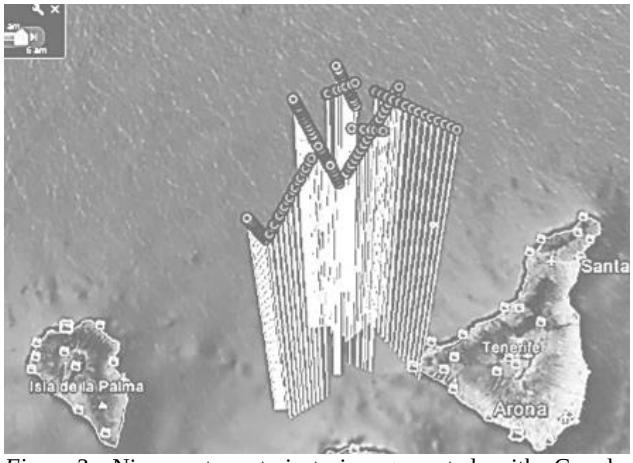

Figure 3 – Nine meteor trajectories generated with Google Earth from the *.kml files. The different dots were derived from meteor information of frames detected by ICC7/ICC9.

For every double-station meteor a *.daf file is generated and named hhmmss.daf (hour, minute, second of the meteor detection). It contains information about all single frames of both cameras at which the meteor is recorded. This includes, amongst others, the time of detection and the position of the meteor which is needed to calculate the meteor's velocity. In *Figure 5* an exemplary *.daf file of a meteor observed on the 6 August 2013 at $03^h03^m09^s$ is shown. The meteor is observed by ICC7 on 17 frames and by ICC9 on 19 frames. For each recorded video frame the file contains information about the meteor as seen by one station. The first column is the consecutive number and the second lists the image time in decimal seconds. In the third column of the table the apparent brightness in magnitudes is noted and the following entries are the relative x and y positions of the meteor in the field of view. The sixth column contains the calculated altitude of the meteor above the Earth's surface and the following the respective error estimate. The latitude and longitude of the point under the meteor are also listed. Furthermore, the distance to the camera in meters with an error estimate is shown in the columns 11 respectively 12. The last two entries present the velocity, as determined for that video frame and the former one, and its error estimate.

With the information of the *.daf files an average velocity is calculated, to reduce the effect of errors in the velocity calculations. The uncertainties are obvious in the last column of *Figure 5* which shows the apparent meteor velocities between two frames. To determine the average velocity, the time interval between the time of the second and the penultimate frame is computed. This way, the majority of the meteor trajectory is utilized. Using the first and the last frame at which a meteor is detected would result in higher uncertainties because in the first frame the meteor is in the process of appearing and in the last frame it is in the process of disappearing. If only 3 frames are available for a recorded meteor, the first and last frames are used to obtain the velocity. Furthermore, the information about the meteor position in longitude and latitude is extracted for those frames from the table. With this it is possible to determine an average velocity. It is calculated for both stations. The mean value of those velocities is utilized in the following. This is done for each double-station meteor. The resulting velocity distribution for all simultaneously detected meteors in the one year is plotted in *Figure 4*. The distribution shows two maxima, one at about 30 km/s and one at about 60 km/s. This differs largely from the theoretical distribution of the former section, which peaks at 12.5 km/s. This measurement bias towards higher velocities will be explained in section 5.

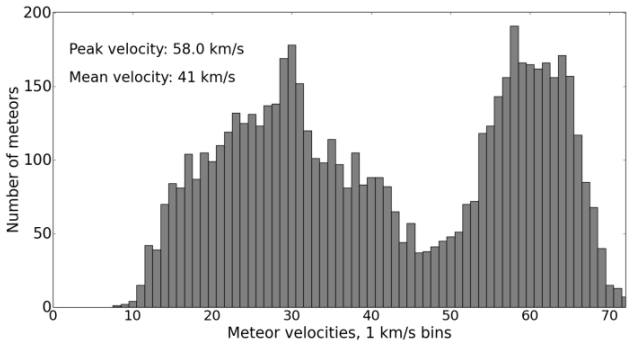

Figure 4 – Velocity distribution of all meteors detected simultaneously by both cameras in the analyzed year in 1 km/s bins.

4 Showers

For further examinations the meteors are sorted by their stream association (sporadic or shower). For this the classification by MetRec for the single station observations is used. Hereafter the Southern Taurids and the Perseids are examined. In the analyzed year 235 Southern Taurids and 149 Perseids were simultaneously detected. *Figure 6* and *Figure 7* show the number of detected Southern Taurids as a function of their velocity. For *Figure 6* only the meteors classified by both cameras as a Southern Taurid were utilized. For *Figure 7*, all meteors which were categorized either by both cameras or only by ICC7 or only by ICC9 as a Southern Taurid were taken. *Figure 8* and *Figure 9* show the same for all meteors related to the Perseids. The known velocities of the showers were extracted from the International Meteor Organization Handbook for Visual Observers (Rendtel, 2014). According to this the Southern Taurids (STA) and the Perseids (PER) have a velocity in free space (v_∞) relative to Earth of:

$$v_{\infty,STA} = 27\ km/s\,, \qquad v_{\infty,PER} = 59\ km/s$$

Figure 6 to Figure 9 also show the peak velocity. The peak velocity is the velocity with the maximum number of observed meteors, derived using the CILBO data. Additionally, the mean velocities of the velocity distributions are calculated.

```
Station 1 - ICC7 - Tenerife
LogFile: 20130805.log
AppearanceDate: 06.08.2013
AppearanceTime: 03:03:09
INFFilename: 030309.inf
FrameCount: 17

!                    Position         Altitude in m            SubPoint        Cam. dist in m  Velocity in km/s
!###   Time  Bright   x      y       h        h            pos   lon/deg  lat/deg     dist   dist     v       v
000   09.31    3.3  0.992  0.898  109052.2  ----.-    56.8   -16.940   28.784   126653.1  ----.-   --.---  --.---
001   09.35    1.5  0.976  0.872  107474.7  ----.-     4.2   -16.950   28.772   125110.9  ----.-   56.028  --.---
002   09.39    0.4  0.960  0.845  105905.7  ----.-    29.8   -16.960   28.760   123599.8  ----.-   58.601  --.---
003   09.43   -0.2  0.943  0.815  104238.1  ----.-    14.3   -16.971   28.748   122019.7  ----.-   62.296  --.---
004   09.47   -0.7  0.926  0.785  102612.9  ----.-     3.8   -16.982   28.735   120507.2  ----.-   57.770  --.---
005   09.51   -1.0  0.909  0.757  101085.0  ----.-    40.8   -16.992   28.724   119110.7  ----.-   57.112  --.---
006   09.55   -1.0  0.892  0.727   99535.8  ----.-    21.8   -17.002   28.712   117721.0  ----.-   55.098  --.---
007   09.59   -0.7  0.873  0.693   97833.7  ----.-    15.9   -17.013   28.699   116224.4  ----.-   63.660  --.---
008   09.63   -0.6  0.853  0.659   96135.5  ----.-     4.7   -17.024   28.686   114765.7  ----.-   60.431  --.---
009   09.67   -0.4  0.834  0.626   94543.8  ----.-    15.1   -17.035   28.674   113430.5  ----.-   59.566  --.---
010   09.71    0.3  0.820  0.602   93404.0  ----.-    14.5   -17.042   28.666   112496.5  ----.-   40.583  --.---

Station 2 - ICC9 - La Palma
LogFile: 20130805.log
AppearanceDate: 06.08.2013
AppearanceTime: 03:03:09
INFFilename: 030309.inf
FrameCount: 19

!                    Position         Altitude in m            SubPoint        Cam. dist in m  Velocity in km/s
!###   Time  Bright   x      y       h        h            pos   lon/deg  lat/deg     dist   dist     v       v
000   09.21    5.1  0.015  0.330  112019.4  ----.-    20.6   -16.920   28.806   145051.9  ----.-   --.---  --.---
001   09.25    4.1  0.031  0.319  110350.9  ----.-    34.2   -16.931   28.794   143045.7  ----.-   60.719  --.---
002   09.29    2.9  0.048  0.308  108636.7  ----.-    13.4   -16.942   28.781   140998.4  ----.-   62.399  --.---
003   09.33    2.1  0.064  0.298  107073.5  ----.-    22.3   -16.952   28.769   139142.9  ----.-   56.922  --.---
004   09.37    1.4  0.082  0.286  105355.2  ----.-    20.7   -16.964   28.756   137118.8  ----.-   62.583  --.---
005   09.41    1.1  0.099  0.274  103764.4  ----.-    12.0   -16.974   28.744   135258.2  ----.-   57.956  --.---
006   09.45    0.6  0.117  0.263  102153.0  ----.-    34.6   -16.985   28.732   133387.8  ----.-   58.726  --.---
007   09.49    0.3  0.136  0.251  100492.4  ----.-    64.9   -16.995   28.719   131476.6  ----.-   60.531  --.---
008   09.53    0.5  0.153  0.239   99031.5  ----.-    22.9   -17.005   28.708   129807.7  ----.-   53.271  --.---
009   09.57    0.8  0.173  0.225   97359.1  ----.-    14.7   -17.016   28.696   127915.4  ----.-   60.997  --.---
010   09.61    1.0  0.194  0.211   95665.5  ----.-    22.2   -17.027   28.683   126018.2  ----.-   61.788  --.---
011   09.65    1.3  0.214  0.198   94103.3  ----.-    16.0   -17.037   28.671   124285.0  ----.-   57.011  --.---
012   09.69    3.4  0.229  0.188   92958.2  ----.-    30.5   -17.045   28.662   123022.9  ----.-   41.799  --.---
```

Figure 5 – Exemplary *.daf file of a meteor observed simultaneously by both cameras on 06 August 2013 at $03^h03^m09^s$.

Figure 6 and *Figure 8* (both stations categorize the meteor as the same stream = bs) yield the following observed peak and mean velocities for the showers:

$$v_{STA,peak,bs} = 29\ km/s, \quad v_{PER,peak,bs} = 58\ km/s$$

$$v_{STA,mean,bs} = 28\ km/s, \quad v_{PER,mean,bs} = 56\ km/s$$

Furthermore, for the velocity distributions of *Figure 7* and *Figure 9* (one or two single-station classification = ss) the peak and mean velocities are computed:

$$v_{STA,peak,ss} = 30\ km/s, \quad v_{PER,peak,ss} = 58\ km/s$$

$$v_{STA,mean,ss} = 29\ km/s, \quad v_{PER,mean,ss} = 55\ km/s$$

These results are quite consistent with the literature values. It has to be taken into account that the meteors near the Earth are accelerated by Earth's gravitation. Additionally, the shower classification is done using the single-station data. This results in higher uncertainties.

To study this in more detail, compare *Figure 6* and *Figure 7*. Both graphs show a similar peak velocity, in agreement with the literature values. However, *Figure 7* (one or two single-station classification) has a higher scattering than *Figure 6* (both cameras categorize the meteor as the same). This shows that most meteors classified as a Southern Taurid by both cameras are quite certain a part of this stream. It also shows, however, that some of the meteors categorized as a Southern Taurid only by one camera are in fact not related to this shower. It follows that the type classification done by MetRec works for the analyzed data, since the peak velocities match the IMO velocities, but is not absolutely reliable, which is reflected by the higher scattering in *Figure 7*.

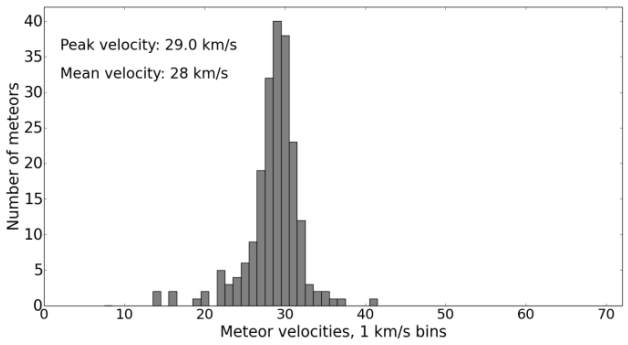

Figure 6 – Velocity distribution of the Southern Taurids detected in one year and classified by both cameras as a Southern Taurid.

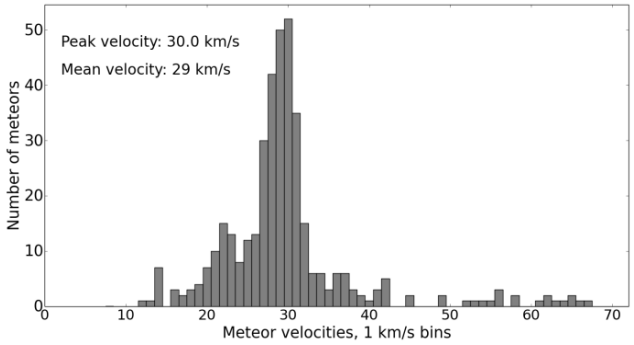

Figure 7 – Velocity distribution of the Southern Taurids detected in one year and classified by at least one of the cameras as a Southern Taurid.

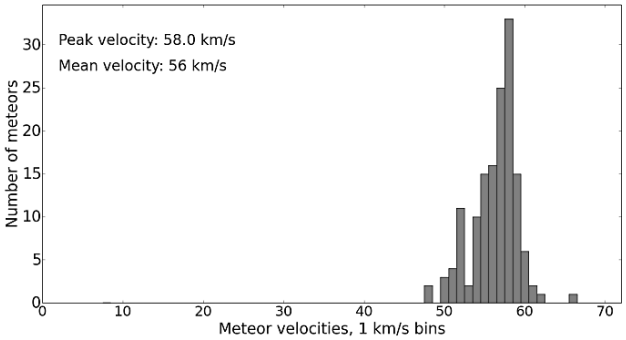

Figure 8 – Velocity distribution of the Perseids detected in one year and classified by both cameras as a Perseid.

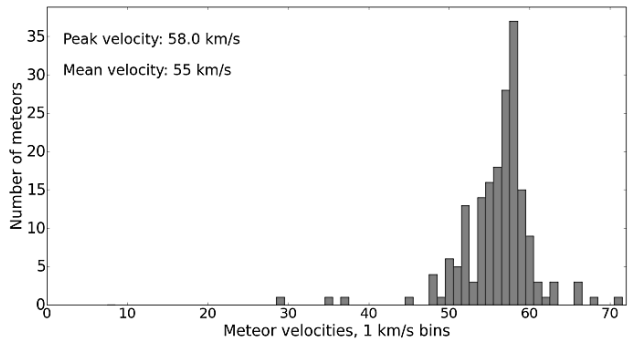

Figure 9 – Velocity distribution of the Perseids detected in one year and classified by at least one of the cameras as a Perseid.

5 Comparison of theory vs. CILBO data

In *Figure 10* the number of detected sporadics as function of their velocity is shown. Only those meteors were utilized which were categorized as sporadics for both camera observations. In *Figure 11* the normalized theoretical velocity distribution for 100 km altitude is shown as a dashed line. Normalizing the sporadic velocity distribution of the CILBO data to one yields the solid line presented in *Figure 11*. The two graphs in this figure are very different. The theoretical line has a high peak at slow velocities around 12.5 km/s. The measured velocities display a more uniform distribution with a minor peak at 64 km/s. This divergence can be attributed to a measuring bias towards higher velocities. The higher the meteor's velocity the brighter the meteor. Due to this the fast meteors can be detected more easily and meteors from smaller and more abundant meteoroids can be detected. Whereas, a lot of slow, faint meteors remain undiscovered.

This relation can be examined if only meteoroids with large masses are analyzed since the brightness of meteors is also proportional to the size of the corresponding meteoroid. The larger the meteoroid, the brighter the meteor. Consequently it is possible to detect large meteoroids even if they are slow. This means that the bias towards high velocities can be minimized if only large meteoroids are analyzed, due to the high detection probability of heavier meteoroids irrespective of their velocity. With the information of the *.daf files the masses of the meteoroids are determined utilizing the mass formula by Verniani (1973):

$$M = 10^{\frac{-m+64.09-10\cdot\log(v)}{2.5}} \qquad (3)$$

Whereas, M is the meteoroid mass outside the Earth's atmosphere, m is the absolute magnitude of the meteor at maximum light and v is the velocity. For a more detailed description see Ott et al. (2014).

We analyzed the velocity distribution, if only meteoroids with a mass $\geq$ 0.5 g are selected which amount to 469 meteors. For these heavier meteoroids the velocity distribution is computed and plotted in *Figure 12*. This graph has its maxima at slower velocities and a steep slope to even smaller and higher velocities. This velocity distribution agrees better with the theoretical expectation than the one calculated for all meteors. *Figure 12* does not show the bias towards higher velocities. This is consistent with the expectations.

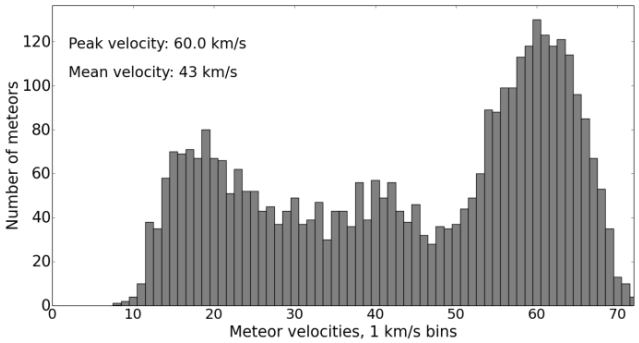

Figure 10 – Velocity distribution of all sporadic meteors detected in one year.

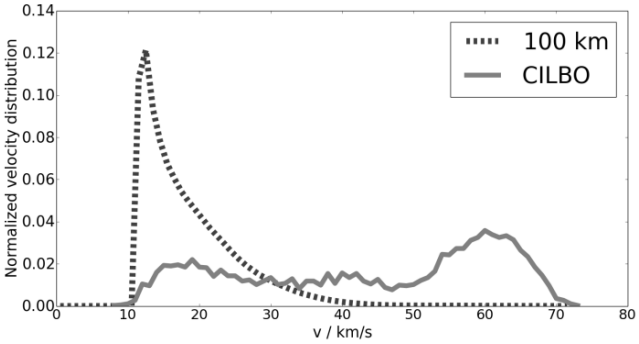

Figure 11 – Normalized theoretical velocity distribution in 100 km above the Earth's surface (dashed line) and the normalized sporadic velocity distribution calculated for one year of CILBO data (solid line).

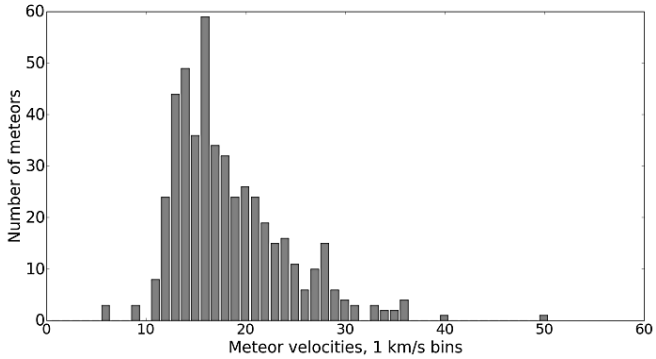

Figure 12 – Velocity distribution of all meteors detected by both cameras in one year with corresponding meteoroid masses $\geq$ 0.5g.

6 The Apex contribution

Figure 10 shows the velocity distribution of all sporadic meteors detected in one year. The maximum number of meteors were determined to have a velocity of about 64 km/s. Since the sporadics cannot be assigned to showers with certain velocities which might be in the 60 km/s category, other reasons for this distinct look must be assumed.

The reason for the high peak around 64 km/s seems to be Earth's rotation in combination with Earth's orbit around the Sun (compare *Figure 13*). At the beginning of the night the observer is located on the back of the Earth with respect to the Earth's direction of movement (A). Consequently, the meteoroids that become visible meteors have to "catch up" with the Earth. Therefore, they reach the Earth's atmosphere with a relatively small velocity. Their lower velocity yields a fainter trail due to less energy and the strong dependence of the meteor brightness on velocity. By contrast, in the early morning hours the observer is located in the front (B). Hence, the meteoroids have a higher velocity with respect to the Earth than the ones in the early evening hours. As a result they cause brighter meteors. Another consequence is that meteors flying from the East to the West move on average faster with respect to the Earth than those from West to East. This is due to the fact that the perceived meteor speed on Earth does not take the speed of the inertial systems, with the observer in the center, into account. This is called the Apex contribution.

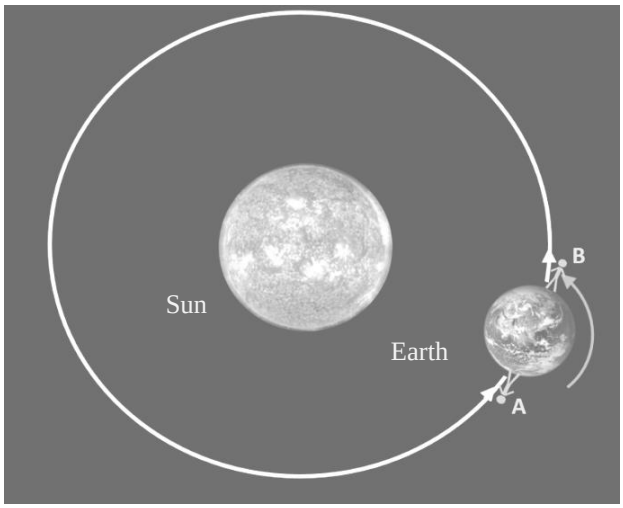

Figure 13 – The Earth orbiting the sun and the Earth's self-rotation. Early evening observations (A) and early morning observations (B).

7 Conclusion and future work

The CILBO data offers a lot of information about the velocities of meteors. The one year double-station data yield information on more than 6000 meteors with usable simultaneous observations.

The shower velocities match the IMO values. An error analysis has to be considered as well as the examination of more showers. Furthermore, the type classification by MetRec works well for the provided data, but is not perfect.

The velocity distribution of the sporadics shows a bias towards higher velocities. This is due to the fact, that the faster the meteor the brighter. Additionally, the larger the meteoroid the brighter the resulting meteor. The velocity distribution of heavier meteoroids is consistent with the theory and has a maximum at 16 km/s. In the future the true velocity distribution of the unbiased measurements should be determined.

Furthermore the sporadic velocity distribution has a peak velocity at about 64 km/s. This peak is a result of the Apex contribution in the early morning hours, when the observer is located in the front of the Earth with respect to the Earth's direction of movement.

References

ECSS (2008). European Cooperation for Space Standardization Space Engineering, Space Environment, ECSS-E-ST-10-04C. Noordwijk, Netherlands: ESA Requirements and Standards Division.

Koschny D., and Diaz del Rio J. (2002). "Meteor Orbit and Trajectory Software (MOTS) - Determining the Position of a Meteor with Respect to the Earth Using Data Collected with the Software MetRec". *WGN, the Journal of the IMO*, **30**, 87–101.

Koschny D., Bettonvil F., Licandro J., van der Luijt C., Mc Auliffe J., Smit H., Svedhem H., de Wit F., Witasse O., and Zender, J. (2013). "A double-station meteor camera setup in the Canary Islands – CILBO". *Geoscientific Instrumentation Methods and Data Systems*, **2**. 339–348.

Koschny D., Mc Auliffe J., Bettonvil F., Drolshagen E., Licandro J., van der Luijt C., Ott T., Smit H., Svedhem H., Witasse O., and Zender, J. (2014). "CILBO - Lessons learnt from a double-station meteor camera setup in the Canary Islands". In Rault J.-L., and Roggemans P., editors, *Proceedings of the International Meteor Conference*, Giron, France, 18–21 September 2014. IMO, pages ???–???.

Molau S. (1999). "The Meteor Detection Software MetRec". In, Baggaley W. J. and Porubcan V., *Proceedings of the International Conference Meteoroids 1998*, 17–21, 1998, Tatranska Lomnica, Slovakia., pages 131–134.

Ott T., Drolshagen E., Koschny D., Drolshagen G., and Poppe B. (2014). "Meteoroid flux determination using imae intensified video camera data from the CILBO double station". In Rault J.-L., and Roggemans P., editors, *Proceedings of the International Meteor Conference*, Giron, France, 18–21 September 2014. IMO, pages ???–???.

Rendtel J. (editor). (2014). Meteor Shower Workbook 2014. IMO.

Taylor A. D. (1995). "The Harvard Radio Meteor Project meteor velocity distribution reappraised". *Icarus*, **116**, 154–158.

Verniani F. (1973). "An Analysis of the Physical Parameters of 5759 Faint Radio Meteors". *Journal of Geophysical Research*, **78**, 8429–8462.